NORTH-HOLLAND
PHYSICS
PUBLISHING

TIME RESPONSE OF ULTRAFAST STREAK CAMERA SYSTEM USING FEMTOSECOND LASER PULSES

P.P. HO, A. KATZ, R.R. ALFANO

Institute for Ultrafast Spectroscopy and Lasers, Photonic Engineering Center, Department of Electrical Engineering, The City College of New York, New York, NY 10031, USA

and

N.H. SCHILLER

Picosecond Streak Camera Application Laboratory, Hamamatsu Corporation, Middlesex, NJ 08846, USA

Received 18 December 1984

Femtosecond laser pulses and dye fluorescence kinetics were used to characterize the time response of an ultrafast streak camera system as a function of an entrance slit.

Reprinted from OPTICS COMMUNICATIONS

TIME RESPONSE OF ULTRAFAST STREAK CAMERA SYSTEM USING FEMTOSECOND LASER PULSES

P.P. HO, A. KATZ, R.R. ALFANO

Institute for Ultrafast Spectroscopy and Lasers, Photonic Engineering Center, Department of Electrical Engineering, The City College of New York, New York, NY 10031, USA

and

N.H. SCHILLER

Picosecond Streak Camera Application Laboratory, Hamamatsu Corporation, Middlesex, NJ 08846, USA

Received 18 December 1984

Femtosecond laser pulses and dye fluorescence kinetics were used to characterize the time response of an ultrafast streak camera system as a function of an entrance slit.

There are several methods available to scientists to measure the ultrafast events on a picosecond and femtosecond time scale. They are the autocorrelation method [1,2], optical Kerr gate [3–5], upconversion gate [6,7], population mixing [8], pump and probe [9,10], and streak camera [11–13]. Each of these techniques has advantages as well as disadvantages. The streak camera method offers the only direct way to measure the intensity profile on a picosecond time scale. The linearly dependence of the detected light intensity in this method avoids the use of nonlinear optical and convolution used in the other detection methods. The main shortcoming of the streak camera is the limitation of the minimum time resolution which depends in part on the size of the input slit. The small slit (~30 μm) limits the amount of light collected and detected by the streak camera system. In this note, we present laser and fluorescence kinetic measurements on the time response dependence of an ultrafast streak camera as a function of the entrance slit width.

A CPM ring dye laser and amplifier system based on the design of Fork et al. [14] was used in this experiment. A laser pulse of 130 fs from the 114 MHz laser oscillator has an output about 200 pJ in energy at 625 nm wavelength. Fig. 1a shows pulse duration measured using the SHG autocorrelation technique [2]. The output power and time duration were stable within a fluctuation of 3%. The laser pulse train was passed into a four-stage dye amplifier system pumped with a frequency doubled Nd:YAG laser at 1 Hz to 10 Hz. The amplified laser pulse had about 1 mJ pulse energy and 0.7 ps pulse duration without pulse compression at 10 Hz rate. The pulse duration for amplified pulse measured by SHG correlation is shown in fig. 1b. A schematic diagram of the laser system is shown in fig. 1c.

A schematic design of the streak camera measurement system is shown in fig. 2. It consists of an input collection optics with adjustable signal input slit width, a temporal disperser with triggering, gating, and ultrafast time sweep high voltage functions, an imaging optics which collects the streaking signal from the phosphorous screen to form an image on the target surface of a SIT vidicon detector, and an optical multichannel analyzer system which records and digitizes the streaking image. All four parts can either increase or reduce the spatial image size of the input signal pulse which may change the time resolution of the detected signal. The magnification factor inside the streaking tube and

0 030-4018/85/$03.30

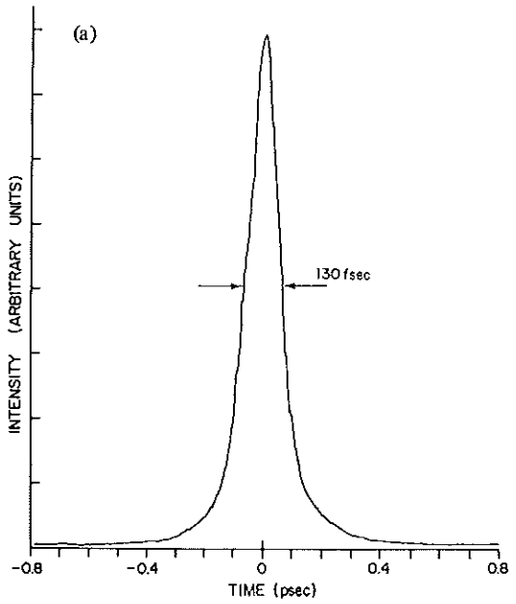

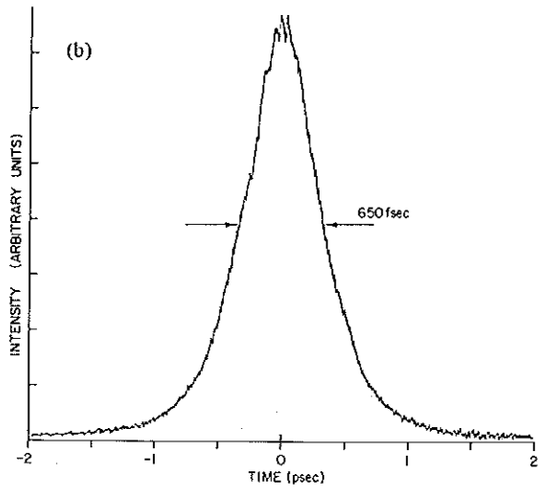

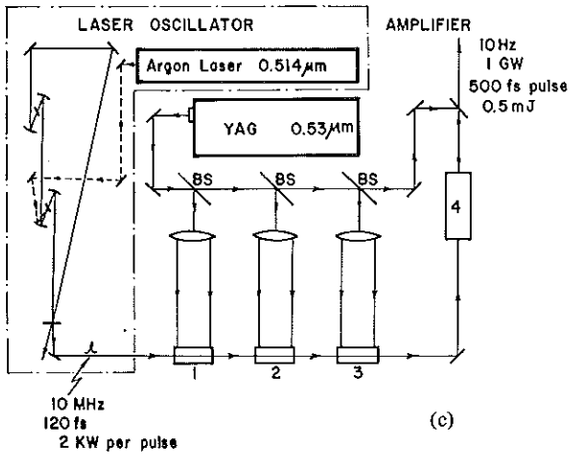

Fig. 1. (a) A typical KDP autocorrelation intensity profile of a CPM ring dye laser. The frequency of the starter was set at 25 Hz. Assuming a $\mathrm{sech}^2(t)$ pulse shape, the duration of the pulses is 130 fs. (b) A KDP autocorrelation intensity profile of the amplified laser pulse. The pulse duration is 650 fs. (c) A schematic diagram of the femtosecond laser system.

the channel width of the vidicon tube are factory determined, and the collation optics and imaging optics are set up before the experiment starts. The input slit width can be adjusted during the experiment to enhance the signal collection efficiency. The performance and the operating characteristics of the Hamamatsu streak camera model HTV C 1370-01 have been described elsewhere [15,16]. It has five streak speeds ranging from 0.21 ns full scale to 65 ns full scale. The minimum time resolution at 10 nm input slit width and 0.21 full scale streak speed is better than 2 ps. The electronic trigger jitter is better than ±20 ps and the signal gain from the five stage signal amplification is about 200. The controllable time resolution factors depend on the input slit width, W, the magnification factor of the collection optics L1(X 1/3), the spot size and magnification factor inside the streak tube (X 1/3), the minimum resolution of the streak width at the output screen (about 71 μm), the magnification factor of the imaging optics L2(X 2), and the resolution of the photo detection system (Temporal analyzer SIT C-1000 has 39 μm width per channel, and the minimum resolution of the streak image is 3 channels). In general, it will be preferred to reduce the input slit width to maintain the minimum time resolution. However, the smaller the input slit width, the smaller the amount of signal photons that can pass through the input slit. In the detection of light emitted from low quantum yield materials, one needs to keep the collection aperture

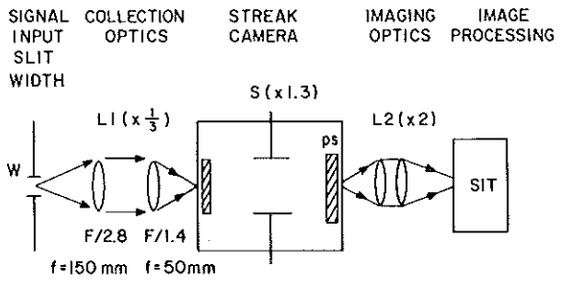

Fig. 2. A block diagram of the image magnification sequence of a streak camera.

and slit as large as possible in order to increase the collect signal level. There is a tradeoff between the input slit size, the collected signal intensity, and the desired ultimate time resolution. In this experiment, we have used the fastest sweeping scale (300 ps full scale) of the streak camera. The intensity profiles in time were measured by a Hamamatsu temporal analyzer minicomputer system.

The time resolution of this system is plotted in fig. 3 as a function of input slit width. Each data point corresponds to an average of about six different measurements. The laser pulse duration 0.4 ps is treated as a δ-function in the analysis in comparison with the time resolution of the streak camera >2 ps. The time scale of the streak camera was calibrated by passing two pulses with known separation distance into the streak camera. A sketched experimental diagram is shown in fig. 4. When the prism was located at position A, the measured channel number separation between the fixed optical path and the variable area optical path was *#a*. After moving the prism into position B, the measured channel number separation between these two optical paths in *#b*, if $A - B = \Delta L/2$, then the measured separation channel numbers *#b* − *#a* from the vidicon were converted into time by using the equation of $\Delta L/c$. For example, $\Delta L = 1$ cm ± 0.001 cm, $c = 3 \times 10^{10}$ cm/s, we obtain the two pulse separation on the vidicon is 85 ± 1 channels. The calibrated value of the streak camera system in this experiment is about 0.39 ± 0.006 ps per TV channel.

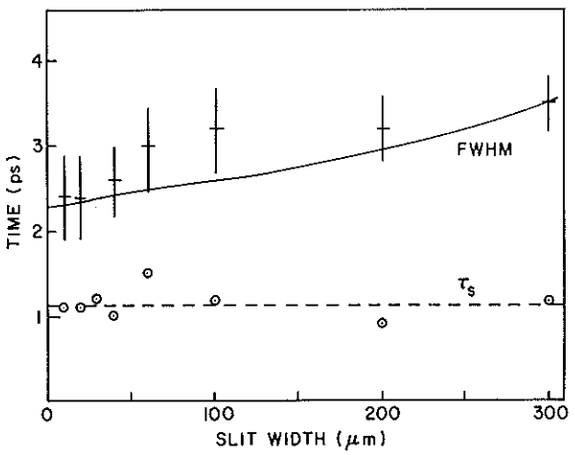

Fig. 3. Time resolution limitation of a streak camera as a function of input slit width. Each data print is an average of about six measurements. The + is the measured average FWHM of a laser pulse. The ○ is the measured average pulse decay slope. The solid line is a calculated curve. The dashed line is a slope decay time $\tau_S = 1.1 \pm 0.2$ ps where $I(t + \tau_S) = (1/e)I(t)$.

The salient feature of the curves in fig. 3 is time resolution of C1370 camera of about 2.5 ± 0.4 ps (FWHM) when the input slit width was below 40 μm and about 3.5 ± 0.3 ps when the input slit width was 300 μm. This data allows the flexibility to choose the input slit width of C1370 streak camera in order to collect more light without worrying about the loss of the time resolution. A calculated curve of the time resolution of the streak camera as a function of the input slit width is plotted as the solid line in fig. 3, by assuming gaussian statistics of the superposition $(\Delta t)^2 = \Sigma_i(\Delta t_i)^2$ the statistical time variation from all possible parameters t_i.

Since most relaxation phenomena in nature can be expressed as exponential or multi-exponential functions, it will be important to present time resolution of the rise time and decay time of a δ-function light pulse profile from the streak camera measurement. When the input slit width was increased, the FWHM of the streak image widened. However, the slope of the rise and decay profiles remained about 1.1 ps ± 0.2 ps. This slope time is plotted as a function of input width as circles in fig. 3. This data suggests that we can widen the input slit width to 300 μm without losing a minimum resolution of 1.1 ps capability in order to measure the relaxation decay associated with an ultrafast decay process. However, the risetime to reach the peak of a widened input slit will be differ-

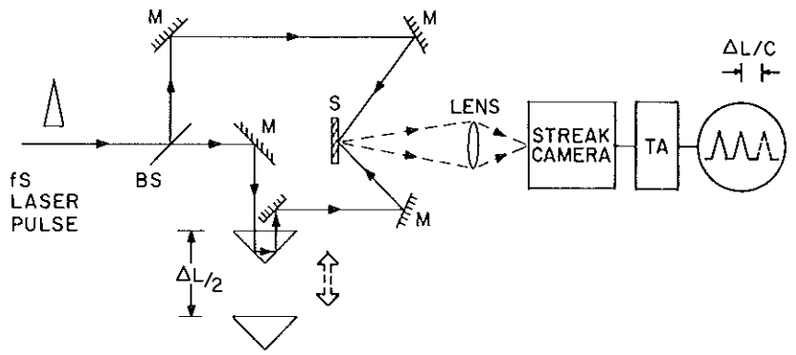

Fig. 4. Time calibration experimental arrangement of the streak camera system. M: mirror, BA: beam splitter, S: scatter plate. ΔL is the controlled distance separation for two different pulse separation times.

ent to that of a narrowed slit because of the excess FWHM of the signal.

The collected signal intensity measured by the streak camera is plotted as a function of the input slit width in fig. 5. The cross symbols represent the integration area of the pulse (peak height × FWHM). All measurements were under the same conditions when the input slit width was widened except the input laser intensity was attentuated by a set of calibrated neutral density filters to avoid the gain saturation of the system. The length of the input slit width was kept the same. The integrated signal intensity was measured to be linearly proportional to the input slit width as shown by the dashed line. At 300 μm entrance slit width, the collection efficiency increased

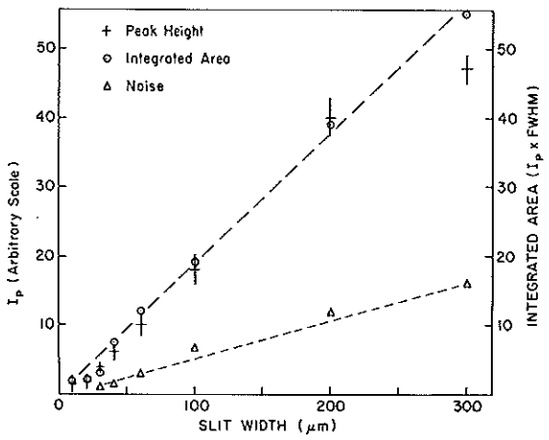

Fig. 5. Collected light intensity and noise of a streak camera as a function of input slit width.

over 20 fold with an overall resolution under 4 ps. The background light level of the streak camera also increased linearly as the input slit width was widened. This data is plotted as the square in fig. 5. The noise can be subtracted from the signal using the electronic microcomputer processing system.

To test the above results, we measured the fluorescence decay kinetics of ultrafast dyes malachite green and crystal violet in water and ethylene glycol solvents. The incident laser power density of the laser pulse at the sample site was varied from 10^8–10^{11} W/cm^2 by controlling the beam spot size at the sample of about 10^{-3} M solution in a 1 mm thickness optical cell. Typical fluorescence intensity decay curves are shown in fig. 6. The mean decay time, τ_D, $[I_F(t_1 + \tau_D) = (1/e)I_F(t_1)]$ for both dyes in water solutions (figs. 6b, 6c) were unresolved on account of the minimum time resolution of the laser pulse and streak camera system (fig. 6a). This indicated the fluorescence decay of these two solutions was less than 2 ps which are confirmed by other published results from the absorption recovery measurement [17].

The fluorescence decay slope for malachite green in ethylene glycol is about 6.1 ± 1.0 ps at 10^8 W/cm^2 excitation intensity. A semilogarithm plot of fig. 6d is displayed in fig. 7. As the input laser intensity is increased tenfold to 10^9 W/cm^2, the measured fluorescence decay time is reduced to 3.9 ± 0.5 ps. Similar results have been obtained in the crystal violet-ethylene glycol solution. At low input excitation laser intensity, the decay time was 7.0 ± 0.9 ps and at higher input laser intensity, the fluorescence decay time is 3.8 ± 0.7 ps. At high intensity excitation experiment, the dye

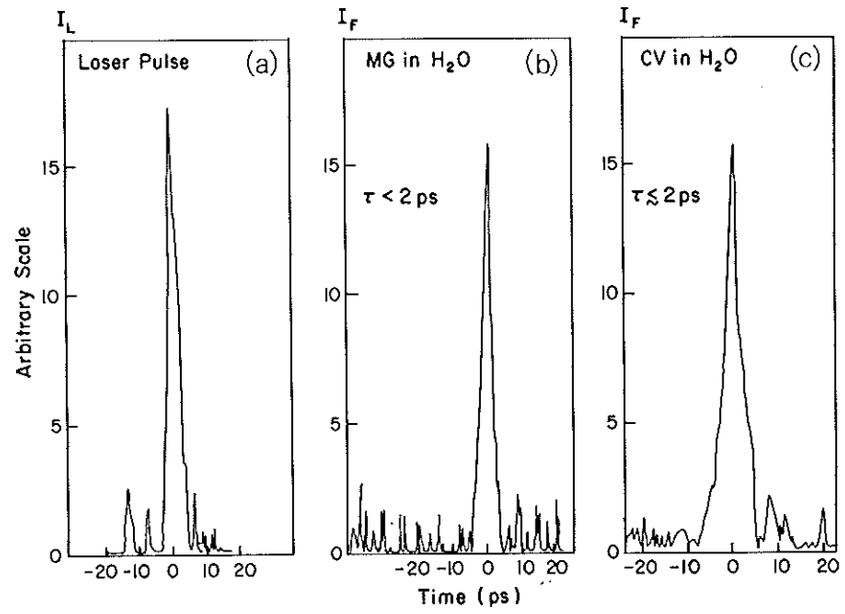

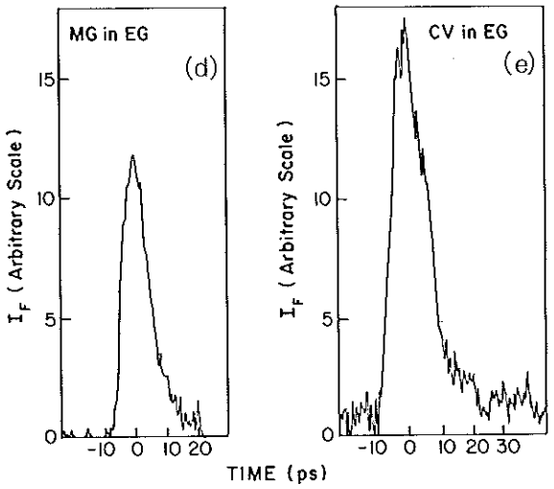

Fig. 6. Fluorescence intensity kinetics of 10^{-3} M ultrafast dyes in solvents at room temperature. The viscosity of the ethylene glycol dye solution was about 15 cp. Input slit width of the streak camera was set at 40 μm. The excitation laser intensity was about 1.2×10^8 W/cm^2. (a) Laser pulse scattered from a metal plate. (b) Malachite green in water. (c) Crystal violet in water. (d) Malachite green in ethylene glycol. (e) Crystal violet in ethylene glycol.

solutions with OD $>$ 10 were bleached during the experiment. A 10^{-3} M dye solution has about 6×10^{14} molecules within a 1 mm^3 volume. The photon number of incident laser pulse with 5×10^8 W/cm^2 intensity and 0.5 ps duration time is about 8×10^{14} 1/cm^2 or flux = $F = 2 \times 10^{27}$ 1/cm^2 s. At this high excitation intensity, the induced emission should be taken into consideration for the measured fluorescence decay time [18,19]. The emission decay time, τ_D', can be expressed as

$$\tau_D' = \tau_D/(1 + W_{21}\tau_D)$$

where W_{21} is the induced emission rate which depends on the input laser excitation intensity [18,19] before the bleaching and τ_D is the fluorescence decay time at low light intensity excitation ($W_{21} \to 0$). From the ab-

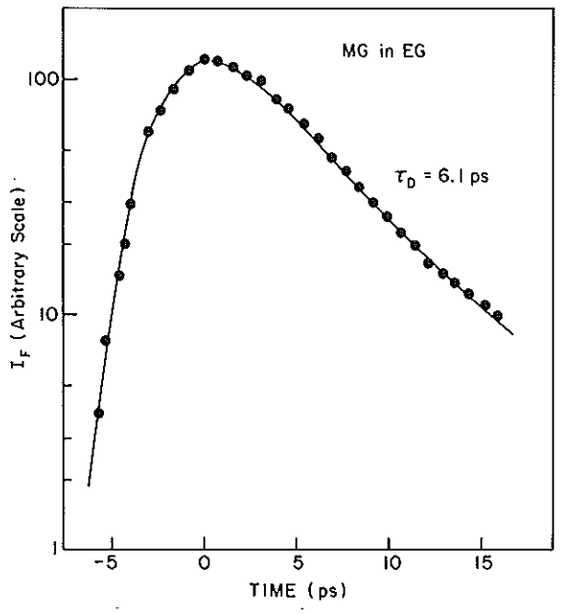

Fig. 7. A semi-logarithm plot of fig. 6d fluorescence decay curve. τ_D = 6.0 ps. The risetime is unresolved from this streak camera system.

sorption recovery time [17] measurement, τ_D (malachite green in ethylene glycol) is about 10 ps. Using our measured results, we can deduce $W_{21}/N \approx 1.6 \times 10^{14}$ 1/mole s where N is the molar concentration of the excited molecules in the dye solution. This implies $\tau_D' \approx 3.8$ ps when input laser intensity exceeds 5×10^8 W/cm^2 at 10^{-3} M solution and $\tau_D' \approx 7.1$ ps at input laser intensity $\approx 10^8$ W/cm^2. The absorption cross section, $\sigma = W/F$, can be deduced from this analysis to be $\approx 10^{-16}$ cm^2.

The time resolution limitation and light collection efficiency of a HTV C1370 streak camera as a function of the input slit width have been demonstrated using a femtosecond laser pulse system. The FWHM of the system time resolution is better than 2.5 ps for slit of 40 μm and 3.5 ps for slit of 300 μm. The decay profile slope is about 1.1 ps for relaxation measurements.

This research at IUSL is funded by AFOSR, PSC-CUNY, and NSF. We thank Y. Budansky for his technical assistance.

References

[1] H.P. Weber, J. Appl. Phys. 39 (1968) 6041.
[2] E.P. Ippen and C.V. Shank, Appl. Phys. Lett. 27 (1975) 488.
[3] M.A. Duguay and J.W. Hansen, Appl. Phys. Lett. 15 (1969) 192.
[4] P.P. Ho and R.R. Alfano, Phys. Rev. A20 (1979) 2170.
[5] C.V. Shank and E.P. Ippen, Appl. Phys. Lett. 26 (1975) 62.
[6] H. Mahr and M.D. Hirsch, Optics Comm. 13 (1975) 96.
[7] Z.Y. Xu and C.L. Tang, Appl. Phys. Lett. 44 (1984) 692.
[8] D. Rosen, A.G. Doukas, Y. Budansky, A. Katz and R.R. Alfano, IEEE QE17 (1981) 2264.
[9] R.R. Alfano and S.L. Shapiro, Phys. Rev. Lett. 26 (1971) 1747.
[10] J.W. Shelton and J. Armstrong, IEEE QE3 (1967) 302.
[11] D.J. Bradley, M.B. Holbrook and W.E. Sleat, IEEE J. QE17 (1981) 658.
[12] F. Pellegrino, A. Dagen and R.R. Alfano, Chem. Phys. 67 (1982) 111.
[13] N.H. Schiller, A. Dagen and R.R. Alfano, Photonic Spectra, March 1982.
[14] R.L. Fork, B.I. Greene and C.V. Shank, Appl. Phys. Lett. 38 (1981) 671.
[15] Y. Tsuchiya, Hamamatsu Tech. Bull. VK1, June (1983).
[16] E. Inuzuka, Y. Tsuchiya, M. Koishi and M. Miwa, Proc. 15th Intern. Congress of High speed photography and photonics, Aug. (1982), San Diego, CA.
[17] E.P. Ippen, C.V. Shank and A. Bergman, Chem. Phys. Lett. 38 (1976) 611.
[18] A.E. Siegmann, Introduction to masers and lasers (McGraw Hill, New York 1971) p. 244.
[19] G.R. Fleming, A.E.W. Knight, J.M. Morris, R.J. Robbins and G.W. Robinson, Chem. Phys. 23 (1977) 61.